

NEXT GENERATION LOSS FUNCTION FOR IMAGE CLASSIFICATION

Shakhnaz Akhmedova 
Centre for Artificial Intelligence in
Public Health Research
Robert Koch Institute
Berlin, Germany
AkhmedovaS@rki.de

Nils Körber
Centre for Artificial Intelligence in
Public Health Research
Robert Koch Institute
Berlin, Germany
KoerberN@rki.de

ABSTRACT

Neural networks are trained by minimizing a loss function that defines the discrepancy between the predicted model output and the target value. The selection of the loss function is crucial to achieve task-specific behaviour and highly influences the capability of the model. A variety of loss functions have been proposed for a wide range of tasks affecting training and model performance. For classification tasks, the cross entropy is the de-facto standard and usually the first choice. Here, we try to experimentally challenge the well-known loss functions, including cross entropy (CE) loss, by utilizing the genetic programming (GP) approach, a population-based evolutionary algorithm. GP constructs loss functions from a set of operators and leaf nodes and these functions are repeatedly recombined and mutated to find an optimal structure. Experiments were carried out on different small-sized datasets CIFAR-10, CIFAR-100 and Fashion-MNIST using an Inception model. The 5 best functions found were evaluated for different model architectures on a set of standard datasets ranging from 2 to 102 classes and very different sizes. One function, denoted as Next Generation Loss (NGL), clearly stood out showing same or better performance for all tested datasets compared to CE. To evaluate the NGL function on a large-scale dataset, we tested its performance on the Imagenet-1k dataset where it showed improved top-1 accuracy compared to models trained with identical settings and other losses. Finally, the NGL was trained on a segmentation downstream task for Pascal VOC 2012 and COCO-Stuff164k datasets improving the underlying model performance.

Keywords Loss function · Genetic Programming · Deep Learning · Classification · Segmentation.

1 Introduction

Deep learning (DL) has received extensive research interest in developing new image processing algorithms, and resulting models have been remarkably successful in a variety of image analysis tasks such as classification Krizhevsky et al. [2012], segmentation Ronneberger et al. [2015], object detection Girshick [2015] and more. Deep learning methods represented by (or partially based on) convolutional neural networks have become a well-known and constantly developing research topic in the field of image analysis. Various deep learning models, for example ResNet He et al. [2015], Inception Szegedy et al. [2015], U-Net Ronneberger et al. [2015], DeepLab Chen et al. [2016], have been proposed over the years for different image processing tasks and domains. Vision transformers Dosovitskiy et al. [2020] constantly gain popularity among researchers due to their high training efficiency and scalability and are already outperforming convolutional neural networks on multiple benchmarks for classification, segmentation and image generation problems.

The loss function plays a crucial role in deep learning in general, as it shows the direction for model training and affects the performance of the model and training speed. There are well-known losses used for most image processing tasks, such as cross entropy (CE) Cover and Thomas [2006], Focal Loss Lin et al. [2017a], or mean square error Willmott and Matsuura [2005]. Recently, researchers started proposing loss functions developed for specific applications or tasks. Usually, that is done by hand and requires a lot of expert knowledge, time, parameter adjustments, and thus computational resources, due to the complexity of modern models.

The loss function design can be represented as a symbolic regression problem that can be solved by using Genetic Programming (GP) Augusto and Barbosa [2000]. The GP approach is frequently used to design previously unknown

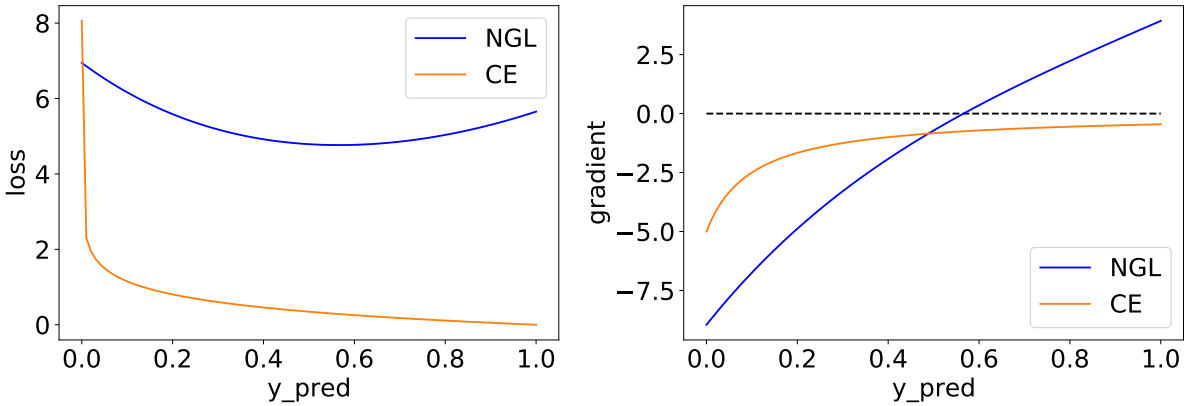


Figure 1: NGL and CE functions (left) and their gradients (right) for $y_{real} = 1$.

heuristics in order to solve hard computational search problems K.Burke et al. [2009]. Genetic programming is a domain-independent method, which was used in this study to genetically breed a population of loss functions for deep learning models to solve image classification problems. GP was applied to find a generally applicable loss function for DL classifiers independent of the dataset and model architecture. Several experiments with different objective functions using InceptionV3 Szegedy et al. [2015] trained on the CIFAR-10 Krizhevsky et al. [2009], Fashion-MNIST Xiao et al. [2017] and CIFAR-100 Krizhevsky et al. [2009] datasets were conducted to find an optimized loss function.

The loss functions found were evaluated using ResNet50 and InceptionV3 models trained on CIFAR-10 Krizhevsky et al. [2009], CIFAR-100 Krizhevsky et al. [2009], Fashion-MNIST Xiao et al. [2017], Malaria Rajaraman et al. [2018], PCam Veeling et al. [2018], Colorectal Histology Kather et al. [2016] and Caltech 101 Fei-Fei et al. [2004] datasets. In the next step, the best function, denoted as NGL, was used to train ResNet He et al. [2015] models and Swin transformers Liu et al. [2021] to classify the ImageNet-1k dataset. In the end, it was applied to train U-Net and DeepLab models on Pascal VOC 2012 Everingham et al. and COCO-Stuff164k Caesar et al. [2018] datasets to show the applicability for segmentation.

Among the evaluated functions, NGL demonstrated exceptionally good results outperforming baseline losses, such as cross entropy loss, focal loss, symmetric cross entropy and dice loss. Moreover, further investigation has showed that the reason for these good results may be self-regulation, which is inherently present in the NGL due to its mathematical definition.

Thus, the main contributions in this paper can be summarized as follows:

- Experimental results show that GP is capable to design a good loss function for deep neural networks without any prior knowledge neither about the model nor about the problem at hand;
- NGL, a new highly efficient loss function, applicable for any DL model to solve classification and segmentation problems, was found;
- Self-regularization naturally implemented in the NGL indicates a direction for loss function design in general;
- Models trained by the NGL achieved same or better performance on a variety of datasets including ImageNet-1k and COCO-Stuff164k datasets.

The rest of this paper is organized as follows. Section 2 briefly reviews related work of deep neural networks used for image analysis and loss function design. The Genetic Programming algorithm and proposed search procedure are described in Section 3, while the experimental settings and results are presented in Section 4. Obtained results are discussed in Section 5. Finally, the paper is concluded in Section 6.

2 Related Work

The progress in solving image processing and visual recognition tasks is related to the rapid development of convolutional neural networks (CNNs) and subsequently vision transformers, which have been already used for real-world applications

in different scientific fields. A plethora of convolutional neural network architectures have been proposed, including the widely used Inception network Szegedy et al. [2014] that explores the problem of multi-scale fusion in convolution calculations to better characterize image information, and ResNet He et al. [2015] with residual blocks to solve the vanishing gradients problem.

Dosovitskiy et al. [2020] proposed the Vision Transformer (ViT) by formulating image classification as a sequence prediction task of the image patch sequence similarly to Vaswani et al. [2017], thereby capturing long-term dependencies within the input image. Transformer-based models for image processing have been rapidly developed, and the following models are considered as some of the most representative: Vision Transformers (ViT) Dosovitskiy et al. [2020], Data-efficient image Transformers (DeiT) Touvron et al. [2020] and Swin-Transformer Liu et al. [2021].

Most deep learning models initially designed to solve classification problems can be applied also for segmentation tasks, as segmentation can be formulated as a classification problem of pixels with semantic labels (semantic segmentation) or partitioning of individual objects (instance segmentation). In the recent decade there were a lot of works presenting new and more powerful segmentation methods, U-Net Ronneberger et al. [2015], which was initially developed for biomedical image segmentation, is one of the most widely used architectures not only in the life sciences. Additionally, DeepLabv1 Chen et al. [2016], DeepLabv2 Chen et al. [2016] and DeepLabv3+ Chen et al. [2018] are among some of the most popular image segmentation approaches, which use dilated convolution to address the decreasing resolution in the network (caused by max-pooling and striding) and Atrous Spatial Pyramid Pooling (ASPP), that probes an incoming convolutional feature layer with filters at multiple sampling rates.

Aside from developing deeper networks with more complex structures and features to get better performance, better loss functions have also been proven to be effective on improving the model performance in most recent works Tian et al. [2022], Jadon [2020]. Many loss functions have been utilized for neural networks based on softmax activation function, such as Mean Square Error (MSE) loss function Willmott and Matsuura [2005], Cross Entropy (CE) loss function Cover and Thomas [2006] (Binary Cross Entropy loss function when images are divided into two classes, Categorical Cross Entropy for multiple classes), etc. In most state-of-the-art supervised learning problems, practitioners typically use large capacity deep neural networks together with cross-entropy loss. The latter can be explained by the fact that the traditional CE loss is supported by clear theory, easy training and good performance. Nowadays, there are many variants of CE that have been proposed in the past few years, e.g. symmetric CE (SCE) Han and Wu [2017], or Focal Loss Lin et al. [2017a].

Loss functions used for segmentation can be divided into four groups described in Jadon [2020]: distribution-based, region-based, boundary-based, and compounded losses. The most well-known and commonly used distribution-based loss functions used to train segmentation models are binary cross entropy Yi-de et al. [2004] and focal loss Lin et al. [2017b]. Region-based loss functions such as dice loss Sudre et al. [2017], and Tversky loss Salehi et al. [2017] calculate the similarity between images. Hausdorff distance loss Ribera et al. [2018] is defined as boundary-based loss functions in Jadon [2020], while the exponential logarithmic loss Wong et al. [2018] is considered as the compounded loss.

Most of the mentioned loss functions can be considered as heuristic methods designed by experts by using theory and the domain knowledge for specific tasks and/or models. Moreover, loss function design requires great effort from experts to explore the large search space, which is usually sub-optimal in practice. Nevertheless, only several commonly used losses are usually implemented for model training, for example, categorical cross entropy for classification or dice loss for segmentation. Recently, the automated search of suitable loss functions without domain knowledge has received much attention from the computer vision community. Reinforcement learning algorithms were used to learn better loss functions with good generalization ability on different image analysis tasks Xu et al. [2018], Oh et al. [2020]. However, loss functions found by using these approaches either have task-specific requirements, such as environment interaction in reinforcement learning, or remain fixed after training.

A lot of works on automatic loss search follow the search algorithms used in AutoML He et al. [2019]. In Li et al. [2021] the authors explore the possibility of searching loss functions automatically from scratch for generic tasks, e.g., semantic and instance segmentation, object detection, and pose estimation. In studies such as Wang et al. [2020] and Li et al. [2019] the main focus is on the search for particular hyper-parameters within the fixed loss formula. AutoML-Zero Real et al. [2020] proposes a framework to construct machine learning algorithms from simple mathematical operations, but the search space and search strategies are specialized, which limits its potential application. The authors of the study presented in Gonzalez and Miikkulainen [2019] propose a framework for searching classification loss functions by using evolutionary algorithms but the searched loss poorly generalizes to large-scale datasets. These works motivated us to design loss functions by using the Genetic Programming algorithm, which uses a large set of primitive mathematical operations and terminal values, capable of training different models regardless of their structure or the task at hand.

3 Method

Genetic Programming (GP) is a population-based evolutionary optimization algorithm, which can be applied to design different heuristics, depending on the problem at hand, and, additionally, it is considered as a machine learning tool, as it can be used to discover a functional relationship between features in data. GP was initially inspired by the biological evolution, including natural processes such as mutation and selection. In GP, each solution is represented by a tree structure, and each of these trees are evaluated recursively to produce the resulting multivariate expression. There are two types of nodes used for tree-based GP: the terminal node, also called leaf, which is randomly chosen from the set of variables, and the tree node, which can be chosen from a predefined set of operators. An example of the generated trees is given in Appendix A (Figure A). The GP search process starts with random initialization of a set of potential solutions, which is also called a population of individuals, in the functional search space. The number of individuals is the predefined parameter n , which does not change through the whole search process. The overall GP search process is summarized in Algorithm 1. Thus, for this study a set of loss functions was randomly generated, and each loss function was represented as a tree, where the terminals were randomly chosen from the set $\{y_{pred}, y_{real}, \mathbb{R}\}$, while the operators were chosen from the set $\{+, -, \times, \div, \times(-1), \sqrt{\cdot}, \log, \exp, \sin, \cos\}$. To utilize these functions and terminals for loss function generation, several modifications were applied (mentioned modifications are described in Appendix A).

Algorithm 1 An overview of the implemented GP approach

```

Randomly initialize  $n$  trees (generation 0), each representing one formula, e.g., loss function
Evaluate GP fitness function  $F$  for each individual in the population
Determine the best individual
Create an empty external archive  $A$ 
while generation number is less than  $T$  do
  for each individual from population do
    Generate a child individual by applying the crossover operator
    if  $rand_1 < M_{ST}$  then
      Apply subtree mutation to the generated child
    end if
    if  $rand_2 < M_N$  then
      Apply one-point mutation to the generated child
    end if
  end for
  Evaluate GP fitness function  $F$  for each generated child individual
  Update the best individual
  Create new population of size  $2 \times n$  by concatenating children and parent individuals
  Select  $n$  best individuals from the new population: create new generation
  Update the external archive  $A$ 
end while

```

After initialization, the main search loop starts, which consists of the iteratively repeated steps crossover, mutation, fitness function evaluation and selection (the number of GP steps or generations is denoted as T). The fitness function F determines the quality of the individual and is the crucial part of the optimization process, as our goal was to experimentally find a robust loss function that can be generalized to a variety of datasets.

The crossover operator is used to exchange the subtrees between two individuals. An example of the implemented crossover operator is demonstrated in Appendix A (Figure A). Mutation can be applied in various ways, but in this study two variants were used:

- a random subtree in the tree is chosen and replaced with another randomly generated subtree (subtree mutation);
- a random node in the tree is chosen and replaced with another randomly generated node (one-point mutation).

Both mutation operators as well as crossover have their own parameters, such as subtree and node mutation M_{ST} , M_N and crossover Cr rates, which determine how often individuals will be changed during the main search loop. Finally, all individuals and the ones generated after crossover and mutation steps are combined into one population, and then the selection operator is applied. In this study only n most fit individuals from the combined population are chosen for the next generation on each GP step.

Moreover, the success-history-based adaptation strategy was used to improve the efficiency of the GP approach. To be more specific, at the beginning of the main search loop an empty external archive A was created. The maximum size of

this archive was set equal to the population size, $n_A = n$. All individuals not passing selection could have been saved in the archive with a given probability p_A . Individuals saved in the external set were used during crossover step with some probability Cr_A .

4 Experiments

4.1 Loss function search

As mentioned in the previous section, loss function search was performed by the GP algorithm and essentially can be described as an optimization process. A set of individuals, where each individual is a mathematical formula representing a loss function, is generated. These individuals change by crossover and mutation operators and then a new set of loss functions is selected. These actions are repeated a given number of times, called generations, and in the end the best individual or loss function is determined. In this implementation, the crucial part is selection, which in turn depends on how the fitness of the loss function is defined, since only the fittest individuals are transferred over to the next generation.

In this study, five experiments were conducted to search the loss function by GP, which only differed in how the fitness function F was defined. Specifically, the following definitions of F were used for each individual loss for each experiment:

- Train the InceptionV3 model from scratch one time on CIFAR-10 dataset, the validation error was used as the fitness value;
- Train the InceptionV3 model from scratch 3 times on Fashion-MNIST dataset, the averaged validation error was used as the fitness value;
- Fine-tune the pre-trained InceptionV3 model one time on CIFAR-10 dataset, the validation error was used as the fitness value;
- Fine-tune the pre-trained InceptionV3 model 3 times on Fashion-MNIST dataset, the averaged validation error was used as the fitness value;
- Train the InceptionV3 model from scratch on CIFAR-10, Fashion-MNIST and CIFAR-100 datasets (once each). The validation error for each dataset was compared to the respective validation error obtained by the same model trained using CE loss, and individual fitness was represented by the pair of numbers indicating the number of wins and the percentage of improvement compared to CE.

It should be noted that a loss function was discarded if its values were not in the range $[10^{-5}, 10^5]$ and a new one was generated instead of it. The fitness function evaluation procedure is described in details in Appendix B.1 (Algorithm B.1).

The model and datasets were selected to limit the training time required per generation while maintaining a reasonable evaluation of the selected loss functions. Regardless of the experiment, a batch size of 128, data augmentation including horizontal flip, width and height shift (0.1 for both), zoom (0.2), Adam optimizer Kingma and Ba [2015] with reduction of the learning rate on plateau, and 50 epochs for CIFAR-10 and CIFAR-100 and 35 for Fashion-MNIST were used to train the network. The top layer of the InceptionV3 model was replaced by 9 new layers, consisting of Flatten, BatchNormalization ($\times 3$) Ioffe and Szegedy [2015], Dense ($\times 3$), Dropout ($\times 2$) Srivastava et al. [2014], and a final Softmax layer.

The following parameters were used for GP regardless of the experiment: $n = 16$, $T = 100$, $M_{ST} = 0.3$, $M_N = 0.1$, $Cr = 0.7$, $p_A = Cr_A = 0.5$, minimum tree height and maximum tree size were set to 2 and 100, respectively.

The best performing functions for each of the five GP experiments were evaluated for different models and multiple datasets, all functions are listed in Appendix B.1.

4.2 Evaluation

4.2.1 Small datasets for classification

The evaluation of the five found functions was performed by training ResNet50 and InceptionV3 on seven datasets, which differed by the number of images, classes, by the type of images (grayscale and RGB), and their sizes. The brief description of datasets used in this study is given in Table 1 (N is the number of classes). ResNet50 was added to the initial experiments, as all the found functions were evaluated on InceptionV3 model during the GP search to rule out model specific properties. The top layers of both InceptionV3 and ResNet50 networks were not included, in both cases instead 9 new layers such as Flatten, BatchNormalization ($\times 3$), Dense ($\times 3$) and Dropout ($\times 2$) were added.

Table 1: Brief description of the small datasets used for classification.

Dataset	N	Dataset size	Class size	Image size	Image type
Malaria	2	27558	13779	edge lengths of 40 – 400 pixels	RGB
PCam	2	327680	163840	96 × 96	RGB
Colorectal Histology	8	5 × 10 ³	625	150 × 150	RGB
CIFAR-10	10	60 × 10 ³	6 × 10 ³	32 × 32	RGB
Fashion-MNIST	10	70 × 10 ³	7 × 10 ³	28 × 28	Grayscale
CIFAR-100	100	60 × 10 ³	6 × 10 ²	32 × 32	RGB
Caltech 101	102	9144	40 – 800	edge lengths of 200 – 300 pixels	RGB

Table 2: Average accuracy (%) for ResNet50 and InceptionV3 each trained 5 times for each dataset for cross entropy (CE) and percentual change of the tested loss functions compared to CE, best result per dataset is shown in bold.

Loss	Malaria	PCam	Colorectal Histology	CIFAR-10	Fashion-MNIST	CIFAR-100	Caltech 101	Mean
CE	94.0	69.4	88.9	92.8	94.0	68.2	72.5	±0
SCE	-0.06	+0.62	-0.45	-3.66	-2.42	-0.80	+2.71	-0.58
Focal	+0.34	+1.03	+ 2.89	-0.64	-0.02	-2.14	-0.78	+0.10
CE + L_2	+0.11	-0.64	+0.88	+0.32	+ 0.09	+0.38	+3.67	+0.69
f_1	-0.27	+0.81	+3.27	-0.34	+0.31	-0.84	-3.67	-0.10
f_2	-0.09	+2.89	-7.56	-0.81	+0.04	+0.60	-3.61	-1.22
f_3	-27.98	+3.24	-62.45	-1.79	-0.48	-59.36	-41.67	-27.21
f_4	-0.21	-0.13	-1.98	-0.14	0.00	-0.32	-6.49	-1.32
$f_5(NGL)$	-0.27	+7.07	+1.77	+0.12	+0.07	+1.01	+5.00	+2.11

Parameter settings and data preprocessing varied for all datasets but were identical for all tested loss functions, specifics are shown in Appendix B.2 (Table B.2.1). Classification accuracy on the test set after the last epoch was used as the evaluation metric.

Both InceptionV3 and ResNet50 models were trained five times for each dataset. Obtained results were averaged for both models and compared to the averaged CE (with and without L_2 regularization), focal and SCE losses for the same models. In the end, the percentage of accuracy improvement or decrease compared to CE was determined. A final value from the range $[-0.5, 0.5]$ was considered as same performing, a value $> +0.5\%$ better performing and $< -0.5\%$ performing worse compared to CE.

Results obtained for all evaluated loss functions used to train models from scratch (f_1, \dots, f_5) are given in Table 2, results obtained for pre-trained models are presented in Appendix B.2 (Table B.2.2). Loss function f_3 demonstrates the worst results compared to others. It showed particularly bad results on Malaria, Colorectal Histology, CIFAR-100, and Caltech 101 datasets, it should be noted that the last three mentioned datasets have less than 10³ examples of each present class. Interestingly, no function outperformed CE loss on Malaria, CIFAR-10, and Fashion-MNIST, while 6 out of 9 functions showed significantly better results on PCam dataset.

Overall, f_5 is the only function showing on average significantly better results than CE, outperforming it on four out of seven datasets with an improvement ranging from 1 to 7%, while there was no significant difference on the remaining three datasets.

Given the overall good performance of the function found by an evolutionary method, we renamed function f_5 as Next Generation Loss (NGL) function, with the following formula:

$$f_{NGL} = \frac{1}{N} \sum_{i=1}^N \left[e^{(\alpha - y_{pred}^{(i)} \cdot (1 + y_{real}^{(i)}))} - \cos(\cos(\sin(y_{pred}^{(i)}))) \right], \tag{1}$$

where $\alpha = 2.4092$, N is the number of classes.

To further test the generalizability of NGL, we tested its performance on ImageNet dataset and larger models.

4.2.2 ImageNet-1k

Experiments on ImageNet-1k dataset were performed using the ResNet He et al. [2015] convolutional neural networks and Swin Liu et al. [2021] transformer models using NGL, CE, SCE and focal losses with the same settings.

Table 3: Comparison of ImageNet results for models trained on CE, SCE NGL and focal losses. †denote results reported as 10-crop testing, all other results show single crop accuracy.

Model	Original top1-acc	Retrained (CE) top1-acc	SCE top1-acc	Focal top1-acc	NGL top1-acc
ResNet101 He et al. [2015]	78.25 †	76.55	77.21	75.68	78.38
ResNet152 He et al. [2015]	78.57 †	76.92	77.51	76.06	78.99
Swin-T Liu et al. [2021]	81.3	81.19	78.79	77.68	81.25
Swin-S Liu et al. [2021]	83.0	83.1	80.68	79.16	83.0

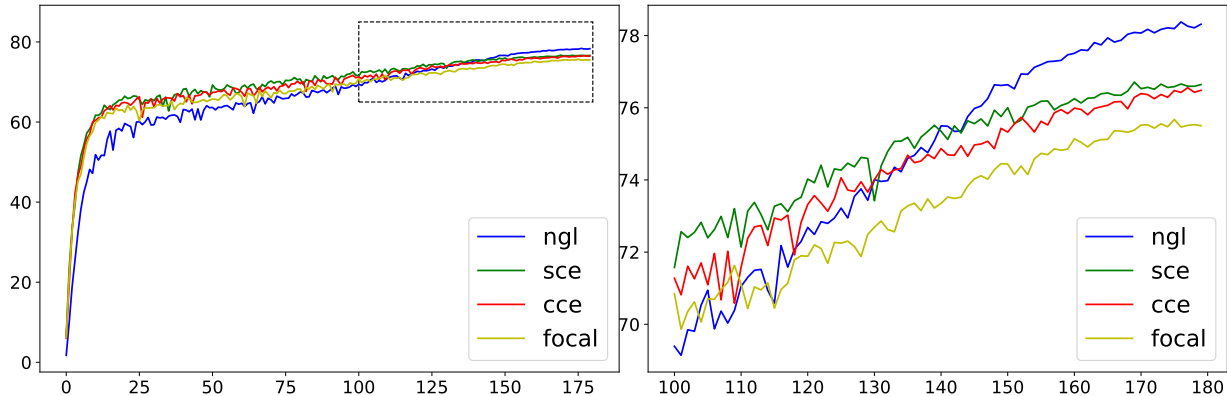


Figure 2: Mean validation accuracy of ResNet101 model on each epoch during ImageNet-1k training.

For ResNet, we used the AdamW optimizer Loshchilov and Hutter [2019], cosine annealing learning rate scheduler with a 30-epoch linear warm-up, while the learning rate was equal to 0.003. The number of epochs was set to 180, a batch size of 256, and a weight decay of 0.01 were used. For Swin-Transformers, the AdamW optimizer was employed for 400 epochs using a cosine decay learning rate scheduler and 60 epochs of linear warm-up. A batch size of 1024, an initial learning rate of 0.001, and a weight decay of 0.05 were used. All of the augmentation and regularization strategies were the same as in Liu et al. [2021]. Results on ImageNet-1k are shown in Table 3. It should be noted, that for both ResNet and Swin models CE was applied with label smoothing and $L2$ regularization.

For ResNet models NGL shows a clear improvement over other losses, increasing the top-1 accuracy by 1 – 3% . For the Swin architecture NGL significantly outperforms SCE and focal losses, while it shows similar performance as regularized CE.

The training process for ResNet101 model is demonstrated in Figure 2. It can be seen that NGL showed slower increase in accuracy compared to other losses, but converges later with a higher accuracy. Even though the NGL was found using only very small datasets, it shows astonishingly good performance on ImageNet-1k. For different architectures and model sizes NGL shows on average superior performance compared to mentioned loss functions.

4.2.3 Segmentation

Additionally, NGL was evaluated on segmentation problems. Specifically, it was used to train two segmentation models, DeepLabv2 with ResNet101 as backbone Nakashima [2018] and U-Net with ResNet34 as backbone. The U-Net model was trained and evaluated only on Pascal VOC 2012 Everingham et al. dataset, while the DeepLabv2 model was used for both Pascal VOC 2012 and COCO-Stuff164k Caesar et al. [2018] datasets.

The first experiments were conducted utilizing the U-Net model. The same parameter setting was used for CE, focal, dice and NGL losses: images were resized to 224×224 , Adam optimizer was applied, the learning rate was 0.0001 and reduced on plateau with a factor of 0.2, patience 5 and $lr_{min} = 10^{-6}$ was used to change it according to the IoU metric value on validation dataset. The model was trained for 100 epochs with a batch size of 32. For DeepLabv2, Adam optimizer was chosen, the learning rate lr was set to 2.5×10^{-5} and the polynomial learning rate scheduler with weight decay 5×10^{-4} and power 0.9 was applied to decrease lr during 2×10^4 iterations. For both models the number of program runs was equal to 5 and mean IoU value was used to evaluate the performance of the model.

Table 4: Comparison of results (mIoU values) on Pascal VOC trained by CE, focal and dice and NGL loss functions.

Model	CE	Focal	Dice	NGL
U-Net	50.1	49.1	46.1	52.8
DeepLabv2	76.7	75.9	74.7	76.7

Table 5: Comparison of results achieved by DeepLabv2 model on COCO-Stuff164k dataset.

	Pixel Accuracy	Mean IoU	Mean Accuracy
CE	66.9	39.8	51.8
Focal	67.7	39.5	51.5
Dice	39.7	17.3	26.9
NGL	67.8	39.9	51.6

Results for Pascal VOC are presented in Table 4. Using the U-Net shows approximately 3 – 7% improvement in terms of mean IoU when NGL is used for training compared to other losses, while showing the same results as CE and outperforming dice and focal losses using DeepLabv2.

Finally, the DeepLabv2 model was trained on COCO-Stuff164k using mentioned loss functions. The parameter setting for these experiments was the same as for Pascal VOC 2012 dataset with the maximum number of iterations set to 3×10^5 . A comparison of results is shown in Table 5, showing slight improvement for NGL loss compared to CE, and significant improvement compared to focal and dice losses.

The obtained results demonstrate that NGL is suitable for downstream segmentation tasks and showing improved performance compared to other commonly used losses.

5 Discussion

For qualitative analysis, the NGL function can be simplified to a binary classification problem, similar as in Gonzalez and Miikkulainen [2019]. For a binary classification problem, NGL is as follows:

$$\begin{aligned}
 f_{NGL} = & \frac{1}{2} \left[e^{(\alpha - y_{pred}^{(0)} \cdot (1 + y_{real}))} + e^{(\alpha - (1 - y_{pred}^{(0)}) \cdot (2 - y_{real}))} \right] \\
 & - \frac{1}{2} \left[\cos(\cos(\sin(y_{pred}^{(0)}))) + \cos(\cos(\sin(1 - y_{pred}^{(0)}))) \right],
 \end{aligned}
 \tag{2}$$

where $\alpha = 2.4092$, $y_{pred} = (y_{pred}^{(0)}, y_{pred}^{(1)})$, $y_{pred}^{(1)} = 1 - y_{pred}^{(0)}$ and $y_{real} \in \{0, 1\}$.

Let us assume that the true labels y_{real} are either 0 or 1. The case where $y_{real} = 1$ is plotted in Figure 1 for the CE loss and NGL functions. The cross entropy shows a monotonic decrease with y_{pred} converging to 1, the NGL shows a decrease in loss, resulting in a minimum at 0.57 and slightly increases when y_{pred} converges to 1. This increase in loss for y_{pred} approaching the true value seems to be counter-intuitive, but may be a factor for the overall good performance of the loss function. The mentioned increase of the loss value may prevent the model from becoming too confident in its output predictions and may provide an important advantage, as it lowers the probability of overfitting. Thus, this could provide an implicit form of regularization, enabling better generalization. A more detailed explanation is given in Appendix C.

While some of the functions found during GP showed better performance on certain datasets, NGL was the only function that performed better than CE (with and without regularization), SCE, focal and dice losses on average and was therefore used for ImageNet-1k and COCO-Stuff164k training, where it was able to show its generalizability to larger datasets and models. The NGL is independent of additional parameters, it is differentiable and has an implicit regularization. For larger datasets it could be observed that it converges slower than other mentioned losses, but at a higher maximum accuracy. The NGL was discovered experimentally and is not supported by theory, which in turn provides less information about the confidence of the model. Nonetheless, for a large proportion of applications the raw performance is the main goal to maximize. The search process did not cover the entire search space and in the future better performing functions may be found, thereby the NGL may point to a promising direction when searching for general suitable functions for classification tasks.

6 Code

Code can be found on the project page <https://github.com/ZKI-PH-ImageAnalysis/Next-Generation-Loss/tree/main>.

7 Conclusions

This study proposes to use Genetic Programming to search a generally applicable loss function for image classification tasks. During that process, a new function was found and shown to outperform other losses, commonly used for classification and segmentation tasks, on average on a variety of datasets demonstrating its general applicability. Moreover, it was shown that proposed loss function can be applied to train a variety of model architectures. Further analysis suggested that improvements provided by the new loss result from implicit regularization that reduces overfitting to the data.

References

- Alex Krizhevsky, Ilya Sutskever, and Geoffrey E Hinton. Imagenet classification with deep convolutional neural networks. *Advances in neural information processing systems*, 25, 2012.
- Olaf Ronneberger, Philipp Fischer, and Thomas Brox. U-net: Convolutional networks for biomedical image segmentation. *ArXiv*, abs/1505.04597, 2015. URL <https://api.semanticscholar.org/CorpusID:3719281>.
- Ross Girshick. Fast r-cnn. In *Proceedings of the IEEE international conference on computer vision*, pages 1440–1448, 2015.
- Kaiming He, X. Zhang, Shaoqing Ren, and Jian Sun. Deep residual learning for image recognition. *2016 IEEE Conference on Computer Vision and Pattern Recognition (CVPR)*, pages 770–778, 2015. URL <https://api.semanticscholar.org/CorpusID:206594692>.
- Christian Szegedy, Vincent Vanhoucke, Sergey Ioffe, Jonathon Shlens, and Zbigniew Wojna. Rethinking the inception architecture for computer vision. *2016 IEEE Conference on Computer Vision and Pattern Recognition (CVPR)*, pages 2818–2826, 2015. URL <https://api.semanticscholar.org/CorpusID:206593880>.
- Liang-Chieh Chen, George Papandreou, Iasonas Kokkinos, Kevin P. Murphy, and Alan Loddon Yuille. Deeplab: Semantic image segmentation with deep convolutional nets, atrous convolution, and fully connected crfs. *IEEE Transactions on Pattern Analysis and Machine Intelligence*, 40:834–848, 2016. URL <https://api.semanticscholar.org/CorpusID:3429309>.
- Alexey Dosovitskiy, Lucas Beyer, Alexander Kolesnikov, Dirk Weissenborn, Xiaohua Zhai, Thomas Unterthiner, Mostafa Dehghani, Matthias Minderer, Georg Heigold, Sylvain Gelly, Jakob Uszkoreit, and Neil Houlsby. An image is worth 16x16 words: Transformers for image recognition at scale. *ArXiv*, abs/2010.11929, 2020. URL <https://api.semanticscholar.org/CorpusID:225039882>.
- Thomas M. Cover and Joy A. Thomas. Elements of information theory (2. ed.). 2006. URL <https://api.semanticscholar.org/CorpusID:702542>.
- Tsung-Yi Lin, Priya Goyal, Ross Girshick, Kaiming He, and Piotr Dollár. Focal loss for dense object detection. In *Proceedings of the IEEE international conference on computer vision*, pages 2980–2988, 2017a.
- Cort J. Willmott and Kenji Matsuura. Advantages of the mean absolute error (mae) over the root mean square error (rmse) in assessing average model performance. *Climate Research*, 30:79–82, 2005. URL <https://api.semanticscholar.org/CorpusID:120556606>.
- D.A. Augusto and H.J.C. Barbosa. Symbolic regression via genetic programming. In *Proceedings. Vol.1. Sixth Brazilian Symposium on Neural Networks*, pages 173–178, 2000.
- Edmund K.Burke, Mathew R. Hyde, Graham Kendall, Gabriela Ochoa, Ender Ozcan, and John R. Woodward. *Exploring Hyper-heuristic Methodologies with Genetic Programming*, pages 177–201. Springer Berlin Heidelberg, Berlin, Heidelberg, 2009.
- Alex Krizhevsky, Geoffrey Hinton, et al. Learning multiple layers of features from tiny images. 2009.
- Han Xiao, Kashif Rasul, and Roland Vollgraf. Fashion-mnist: a novel image dataset for benchmarking machine learning algorithms, 2017.
- Sivaramkrishnan Rajaraman, Sameer K Antani, Mahdieh Poostchi, Kamolrat Silamut, Md A Hossain, Richard J Maude, Stefan Jaeger, and George R Thoma. Pre-trained convolutional neural networks as feature extractors toward improved malaria parasite detection in thin blood smear images. *PeerJ*, 6:e4568, 2018.
- Bastiaan S Veeling, Jasper Linmans, Jim Winkens, Taco Cohen, and Max Welling. Rotation equivariant CNNs for digital pathology. June 2018.
- Jakob Nikolas Kather, Cleo-Aron Weis, Francesco Bianconi, Susanne M Melchers, Lothar R Schad, Timo Gaiser, Alexander Marx, and Frank Gerrit Zöllner. Multi-class texture analysis in colorectal cancer histology. *Scientific reports*, 6:27988, 2016.

- Li Fei-Fei, Rob Fergus, and Pietro Perona. Learning generative visual models from few training examples: An incremental bayesian approach tested on 101 object categories. *Computer Vision and Pattern Recognition Workshop*, 2004.
- Ze Liu, Yutong Lin, Yue Cao, Han Hu, Yixuan Wei, Zheng Zhang, Stephen Lin, and Baining Guo. Swin transformer: Hierarchical vision transformer using shifted windows. In *Proceedings of the IEEE/CVF International Conference on Computer Vision (ICCV)*, 2021.
- M. Everingham, L. Van Gool, C. K. I. Williams, J. Winn, and A. Zisserman. The PASCAL Visual Object Classes Challenge 2012 (VOC2012) Results. <http://www.pascal-network.org/challenges/VOC/voc2012/workshop/index.html>.
- Holger Caesar, Jasper Uijlings, and Vittorio Ferrari. Coco-stuff: Thing and stuff classes in context. In *Computer vision and pattern recognition (CVPR), 2018 IEEE conference on*. IEEE, 2018.
- Christian Szegedy, Wei Liu, Yangqing Jia, Pierre Sermanet, Scott E. Reed, Dragomir Anguelov, D. Erhan, Vincent Vanhoucke, and Andrew Rabinovich. Going deeper with convolutions. *2015 IEEE Conference on Computer Vision and Pattern Recognition (CVPR)*, pages 1–9, 2014. URL <https://api.semanticscholar.org/CorpusID:206592484>.
- Ashish Vaswani, Noam M. Shazeer, Niki Parmar, Jakob Uszkoreit, Llion Jones, Aidan N. Gomez, Lukasz Kaiser, and Illia Polosukhin. Attention is all you need. In *NIPS*, 2017. URL <https://api.semanticscholar.org/CorpusID:13756489>.
- Hugo Touvron, Matthieu Cord, Matthijs Douze, Francisco Massa, Alexandre Sablayrolles, and Hervé Jégou. Training data-efficient image transformers & distillation through attention. In *International Conference on Machine Learning*, 2020. URL <https://api.semanticscholar.org/CorpusID:229363322>.
- Liang-Chieh Chen, Yukun Zhu, George Papandreou, Florian Schroff, and Hartwig Adam. Encoder-decoder with atrous separable convolution for semantic image segmentation. In *ECCV*, 2018.
- Yingjie Tian, Duo Su, Stanislao Lauria, and Xiaohui Liu. Recent advances on loss functions in deep learning for computer vision. *Neurocomputing*, 497:129–158, 2022. URL <https://api.semanticscholar.org/CorpusID:248642142>.
- Shruti Jadon. A survey of loss functions for semantic segmentation. *2020 IEEE Conference on Computational Intelligence in Bioinformatics and Computational Biology (CIBCB)*, pages 1–7, 2020. URL <https://api.semanticscholar.org/CorpusID:220128180>.
- Bin Han and Yiquan Wu. A novel active contour model based on modified symmetric cross entropy for remote sensing river image segmentation. *Pattern Recognit.*, 67:396–409, 2017. URL <https://api.semanticscholar.org/CorpusID:2500127>.
- Ma Yi-de, Liu Qing, and Qian Zhi-bai. Automated image segmentation using improved pcnn model based on cross-entropy. *Proceedings of 2004 International Symposium on Intelligent Multimedia, Video and Speech Processing, 2004.*, pages 743–746, 2004. URL <https://api.semanticscholar.org/CorpusID:11039022>.
- Tsung-Yi Lin, Priya Goyal, Ross B. Girshick, Kaiming He, and Piotr Dollár. Focal loss for dense object detection. *2017 IEEE International Conference on Computer Vision (ICCV)*, pages 2999–3007, 2017b. URL <https://api.semanticscholar.org/CorpusID:47252984>.
- Carole Helene Sudre, Wenqi Li, Tom Kamiel Magda Vercauteren, Sébastien Ourselin, and M. Jorge Cardoso. Generalised dice overlap as a deep learning loss function for highly unbalanced segmentations. *Deep learning in medical image analysis and multimodal learning for clinical decision support : Third International Workshop, DLMIA 2017, and 7th International Workshop, ML-CDS 2017, held in conjunction with MICCAI 2017 Quebec City, QC,...*, 2017:240–248, 2017. URL <https://api.semanticscholar.org/CorpusID:21957663>.
- Seyed Sadegh Mohseni Salehi, Deniz Erdoğan, and Ali Gholipour. Tversky loss function for image segmentation using 3d fully convolutional deep networks. In *MLMI@MICCAI*, 2017. URL <https://api.semanticscholar.org/CorpusID:732793>.
- Javier Ribera, David Güera, Yuhao Chen, and Edward J. Delp. Weighted hausdorff distance: A loss function for object localization. *ArXiv*, abs/1806.07564, 2018. URL <https://api.semanticscholar.org/CorpusID:49322181>.
- Ken C. L. Wong, Mehdi Moradi, Hui Tang, and Tanveer F. Syeda-Mahmood. 3d segmentation with exponential logarithmic loss for highly unbalanced object sizes. *ArXiv*, abs/1809.00076, 2018. URL <https://api.semanticscholar.org/CorpusID:52157209>.
- Zhongwen Xu, H. V. Hasselt, and David Silver. Meta-gradient reinforcement learning. In *Neural Information Processing Systems*, 2018. URL <https://api.semanticscholar.org/CorpusID:43966764>.
- Junhyuk Oh, Matteo Hessel, Wojciech M. Czarnecki, Zhongwen Xu, H. V. Hasselt, Satinder Singh, and David Silver. Discovering reinforcement learning algorithms. *ArXiv*, abs/2007.08794, 2020. URL <https://api.semanticscholar.org/CorpusID:220633409>.
- Xin He, Kaiyong Zhao, and Xiaowen Chu. Automl: A survey of the state-of-the-art. *ArXiv*, abs/1908.00709, 2019. URL <https://api.semanticscholar.org/CorpusID:199405568>.
- Hao Li, Tianwen Fu, Jifeng Dai, Hongsheng Li, Gao Huang, and Xizhou Zhu. Autoloss-zero: Searching loss functions from scratch for generic tasks. *2022 IEEE/CVF Conference on Computer Vision and Pattern Recognition (CVPR)*, pages 999–1008, 2021. URL <https://api.semanticscholar.org/CorpusID:232352674>.
- Xiaobo Wang, Shuo Wang, Cheng Chi, Shifeng Zhang, and Tao Mei. Loss function search for face recognition. *ArXiv*, abs/2007.06542, 2020. URL <https://api.semanticscholar.org/CorpusID:220496317>.

- Chuming Li, Chen Lin, Minghao Guo, Wei Wu, Wanli Ouyang, and Junjie Yan. Am-lfs: Automl for loss function search. *2019 IEEE/CVF International Conference on Computer Vision (ICCV)*, pages 8409–8418, 2019. URL <https://api.semanticscholar.org/CorpusID:158046703>.
- Esteban Real, Chen Liang, David R. So, and Quoc V. Le. Automl-zero: Evolving machine learning algorithms from scratch. In *International Conference on Machine Learning*, 2020. URL <https://api.semanticscholar.org/CorpusID:212634211>.
- Santiago Gonzalez and Risto Miikkulainen. Improved training speed, accuracy, and data utilization through loss function optimization. *2020 IEEE Congress on Evolutionary Computation (CEC)*, pages 1–8, 2019. URL <https://api.semanticscholar.org/CorpusID:167217832>.
- Diederik P. Kingma and Jimmy Ba. Adam: A method for stochastic optimization. In Yoshua Bengio and Yann LeCun, editors, *3rd International Conference on Learning Representations, ICLR 2015, San Diego, CA, USA, May 7-9, 2015, Conference Track Proceedings*, 2015. URL <http://arxiv.org/abs/1412.6980>.
- Sergey Ioffe and Christian Szegedy. Batch normalization: Accelerating deep network training by reducing internal covariate shift. In *International Conference on Machine Learning*, 2015. URL <https://api.semanticscholar.org/CorpusID:5808102>.
- Nitish Srivastava, Geoffrey Hinton, Alex Krizhevsky, Ilya Sutskever, and Ruslan Salakhutdinov. Dropout: A simple way to prevent neural networks from overfitting. *Journal of Machine Learning Research*, 15(56):1929–1958, 2014.
- Ilya Loshchilov and Frank Hutter. Decoupled weight decay regularization, 2019.
- Kazuto Nakashima. deeplab-pytorch. <https://github.com/kazuto1011/deeplab-pytorch>, 2018.

A Method

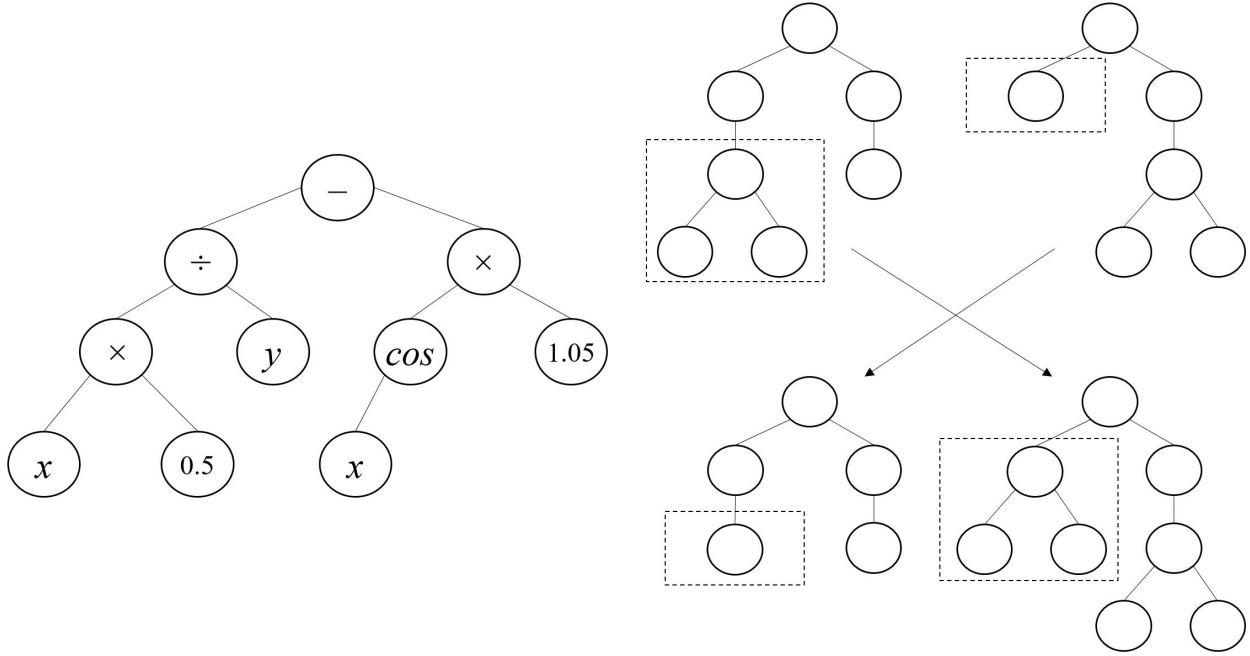


Figure A: Left: an example of the solution representation for tree-based GP: $\frac{0.5 \times x}{y} - 1.05 \times \cos(x)$. Right: an example of the subtrees exchange during crossover.

The GP search process starts with random initialization of a set of potential solutions, which is also called a population of individuals, in the functional search space. For this study a set of loss functions was randomly generated, and each loss function was represented as a tree, where the terminals were randomly chosen from the set $\{y_{pred}, y_{real}, \mathbb{R}\}$, while the operators were chosen from the set $\{+, -, \times, \div, \times(-1), \sqrt{\cdot}, \log, \exp, \sin, \cos\}$. To utilize these functions and terminals for loss function generation, the following modifications were applied:

- $x \div y$ was changed to $x \div (y + \varepsilon)$;
- \sqrt{x} was changed to $\sqrt{|x| + \varepsilon}$;
- $\log(x)$ was changed to $\log(|x| + \varepsilon)$, with $\varepsilon = 10^{-8}$;
- it was implemented as a rule that both y_{pred} and y_{real} should be present in the formula, and $y_{pred} \in [0, 1]$ (Softmax is always the last layer of the model).

B Experiments

B.1 Loss function search

In this study, five experiments were conducted to search the loss function by GP, which only differed in how the fitness function F was defined. Specifically, the following definitions of F were used for the respective experiments:

- each individual loss function was used to train the InceptionV3 model from scratch one time on CIFAR-10 dataset, the validation error was used as the fitness value;
- each individual loss function was used to train the InceptionV3 model from scratch 3 times on Fashion-MNIST dataset, the averaged validation error was used as the fitness value;
- each individual loss function was used to fine-tune the pre-trained InceptionV3 model one time on CIFAR-10 dataset, the validation error was used as the fitness value;
- each individual loss function was used to fine-tune the pre-trained InceptionV3 model 3 times on Fashion-MNIST dataset, the averaged validation error was used as the fitness value;

- each individual loss function was used to train the InceptionV3 model from scratch on CIFAR-10, Fashion-MNIST and CIFAR-100 datasets (once each). The validation error for each dataset was compared to the respective validation error obtained by the same model trained using CE loss, and individual fitness was represented by the pair of numbers indicating the number of wins and the percentage of improvement compared to CE.

For the first four experiments, the classification error was used to evaluate individual's fitness, and, therefore, the individual with the smallest classification error was considered as the best one. However, for the last experiment, individuals were compared in the following way:

- if individual f_i outperformed CE at least once and individual f_j showed worse results on all 3 datasets, then f_i was considered as the better loss function;
- if both individuals f_i and f_j outperformed CE the same number of times, then the mean percentage of improvement for all winning datasets was calculated and the loss with higher mean value was considered as the better one;
- if both individuals f_i and f_j showed worse results on all datasets compared to the CE loss, then the one with lower mean second value was considered as the better loss.

The fitness function F evaluation procedure for all 5 experiments is described in Algorithm B.1. It should be noted that in Algorithm B.1 the number of datasets was set to 1 for the first 4 experiments and 3 for the last one. Besides, the number of runs was equal to 1 for the first, third and last experiments, while it was set to 3 for the remaining experiments.

Algorithm B.1 Fitness function F evaluation

Require: Test error values of the InceptionV3 model trained by using CE on all given datasets

```

for each individual from population do
  for each dataset used for a given experiment do
    for each run do
      Randomly generate train, val and test sets
      Create an InceptionV3 model
      Train the model for a given number of epochs
      Evaluate model's accuracy on the test set
      if only one dataset is used for an experiment then
        Save model's test error
      else
        Determine whether individual outperformed CE or not
        Save the percentage of improvement compared to CE
      end if
    end for
    if only one dataset is used for an experiment then
      Save individual's test error averaged over all runs
    else
      Calculate individual's number of wins compared to CE
      Calculate the average percentage of improvement compared to CE
    end if
  end for
  if only one dataset is used for an experiment then
    Save individual's averaged test error
  else
    Save the number of wins and average percentage of improvement as a pair of values
  end if
end for
    
```

The best performing functions for each of the five GP experiments are listed below:

$$f_1 = \frac{1}{N} \sum_{i=1}^N \frac{e^{(\sin^2(y_{pred}^{(i)}))}}{2 \times (|\beta - y_{real}^{(i)}| \times y_{pred}^{(i)} + \varepsilon)}, \quad (\text{B.1.1})$$

Table B.2.1: Parameter settings for used small datasets.

	CIFAR-10	Fashion-MNIST	CIFAR-100	Malaria	PCam	Caltech 101	Colorectal Histology
Epochs	200	100	200	400	50	400	600
Optimizer	Adam: $\beta_1 = 0.9, \beta_2 = 0.999, \epsilon = 10^{-7}$				SGD: momentum 0.9		
Learning rate lr	0.001				0.01		
Scheduler	Reduce on Plateau: factor 0.2, patience 5, $lr_{min} = 10^{-4}$						
Batch size	128		32		128	32	
Image size	32×32	224×224		75×75	96×96	224×224	150×150
Augmentation	Zoom 0.2, width and height shift (0.1 for both), horizontal flip						

Table B.2.2: Average accuracy (%) for pre-trained ResNet50 and InceptionV3 each fine-tuned 5 times for each dataset for cross entropy (CE) and percentual change of the tested loss functions compared to CE, best result per dataset is shown in bold.

Loss	Malaria	PCam	Colorectal Histology	CIFAR-10	Fashion-MNIST	CIFAR-100	Caltech 101	Mean
CE	96.7	72.4	90.5	94.9	94.6	74.8	84.5	± 0
SCE	+0.11	-0.83	-2.13	-2.12	-1.82	-1.25	-0.02	-1.13
Focal	+0.15	+3.86	+2.44	+0.35	+0.08	-3.18	+0.52	+0.58
CE + L_2	+0.34	+0.73	-2.77	+0.50	-0.08	-0.23	-1.19	-0.39
f_1	+0.20	+7.90	+5.33	-1.33	-0.17	+2.89	-0.33	+2.06
f_2	-0.09	+8.62	+4.54	+0.19	+0.09	+4.79	+0.10	+2.61
f_3	-2.13	+0.51	-50.96	+1.74	-0.04	+4.98	+5.59	-5.76
f_4	-0.04	+8.10	+3.03	+0.02	-0.13	+6.78	+5.47	+3.33
$f_5(NGL)$	-0.26	+7.07	+5.01	-0.37	-0.30	+5.29	+3.45	+2.84

$$f_2 = \frac{1}{N} \sum_{i=1}^N \left[\frac{\cos(-y_{real}^{(i)})}{\sqrt{|y_{pred}^{(i)}| + \varepsilon + \varepsilon}} \times (y_{pred}^{(i)} - \gamma) + (y_{pred}^{(i)})^4 + \sqrt{|y_{real}^{(i)} + y_{pred}^{(i)}| + \varepsilon} \right], \quad (\text{B.1.2})$$

$$f_3 = \frac{1}{N} \sum_{i=1}^N \sqrt{\left| \frac{y_{real}^{(i)}}{\sin(y_{real}^{(i)}) + \varepsilon} + \frac{y_{pred}^{(i)} - e^\delta}{\zeta} \right| + \varepsilon}, \quad (\text{B.1.3})$$

$$f_4 = \frac{1}{N} \sum_{i=1}^N \sin(\sin(y_{pred}^{(i)} - \eta) + (y_{real}^{(i)})^3), \quad (\text{B.1.4})$$

$$f_5 = NGL = \frac{1}{N} \sum_{i=1}^N \left[e^{(\alpha - y_{pred}^{(i)} - y_{pred}^{(i)} \times y_{real}^{(i)})} - \cos(\cos(\sin(y_{pred}^{(i)}))) \right], \quad (\text{B.1.5})$$

where $\alpha = 2.4092$, $\beta = 1.5494$, $\gamma = 3.8235$, $\delta = 3.1868$, $\zeta = 2.4428$, $\eta = 2.6085$, $\varepsilon = 10^{-8}$ and N is the number of classes. Here in all formulas $y_{pred} = (y_{pred}^{(1)}, \dots, y_{pred}^{(N)})$ is obtained after applying softmax function to the generated prediction, thus, $y_{pred}^{(i)} \in [0, 1], i \in [1, N]$. Later in the study f_5 was denoted as NGL .

B.2 Small datasets

Parameter settings and data preprocessing varied for all datasets but were identical for all tested loss functions, specifics are shown in Table B.2.1. Classification accuracy on the test set after the last epoch was used as the evaluation metric.

The evaluation of the five found functions was performed by training ResNet50 and InceptionV3 on seven datasets, which differed by the number of images, classes, by the type of images (grayscale and RGB), and their sizes. Classification accuracy on the test set after the last epoch was used as the evaluation metric. Both InceptionV3 and ResNet50 models were trained five times for each dataset. Obtained results were averaged for both models and compared to the averaged CE loss for the same models. In the end, the percentage of accuracy improvement or decrease compared to CE was determined. A final value from the range $[-0.5, 0.5]$ was considered as same performing, a value $> +0.5\%$ better performing and $< -0.5\%$ performing worse compared to CE. Here results obtained for all five evaluated loss functions (f_1, \dots, f_5) used to fine-tune pre-trained ResNet50 and InceptionV3 models are given in Table B.2.2.

C Discussion

All functions found by GP and listed in Section 1.1 were analysed the same way as was done in Gonzalez and Miikkulainen [2019], thus, they were analysed in the context of binary classification to show why and how they work. For example, let us consider loss function NGL for classification problem with $N = 2$ classes:

$$NGL = \frac{1}{2} \left[e^{(\alpha - y_{pred}^{(0)} \cdot (1 + y_{real}^{(0)}))} + e^{(\alpha - y_{pred}^{(1)} \cdot (1 + y_{real}^{(1)}))} \right] - \frac{1}{2} \left[\cos(\cos(\sin(y_{pred}^{(0)}))) + \cos(\cos(\sin(y_{pred}^{(1)}))) \right], \quad (\text{B.2.1})$$

where $\alpha = 2.4092$.

Since vectors y_{pred} and y_{real} sum to 1, by consequence of being passed through a softmax function, for binary classification $y_{pred} = (y_{pred}^{(0)}, 1 - y_{pred}^{(0)})$ and $y_{real} = (y_{real}^{(0)}, 1 - y_{real}^{(0)})$. This constraint simplifies the binary NGL loss to the following function of two variables $(y_{pred}^{(0)}, y_{real}^{(0)})$:

$$NGL = \frac{1}{2} \left[e^{(\alpha - y_{pred}^{(0)} \cdot (1 + y_{real}^{(0)}))} + e^{(\alpha - (1 - y_{pred}^{(0)}) \cdot (2 - y_{real}^{(0)}))} \right] - \frac{1}{2} \left[\cos(\cos(\sin(y_{pred}^{(0)}))) + \cos(\cos(\sin(1 - y_{pred}^{(0)}))) \right], \quad (\text{B.2.2})$$

where $\alpha = 2.4092$. This same methodology can be applied to the cross-entropy loss and other functions found by GP and listed in Section 2.1.

Let us assume that true labels y_{real} are either 0 or 1. The case where $y_{real} = 1$ is plotted in Fig. B.2 for the CE loss and loss functions found by GP. The cross-entropy and f_3 losses are shown to be monotonically decreasing, f_2 loss has a small region where it increases and after that, similar to CE and f_3 , it starts to decrease, while the remaining three functions, f_1 , f_4 and NGL , show an increase in the loss value as the predicted label, y_{pred} , approaches the true label y_{true} . This increase of the loss value allows the loss functions f_1 , f_4 and NGL to prevent the model from becoming too confident in its output predictions. The latter may provide an important advantage as it lowers the probability of network's overfitting. Thus, these loss functions provide an implicit form of regularization, enabling better generalization.

Results, achieved on small datasets, show that the only found function, which monotonically decreases, f_3 , demonstrates worst results as for models trained from scratch and for pretrained models. Loss f_2 shows almost the same results as CE on most of small datasets, but is significantly worse on datasets such as Colorectal Histology and Caltech101. Despite the fact that generally results for f_1 are good, it should be noted that function f_1 (similarly to f_2) depends on the ε value, which has significant impact on the value of f_1 itself and makes the latter differentiable. Therefore, only functions f_4 and NGL have the mentioned form of regularization and do not depend on additional parameters such as introduced ε value. It can be seen from Fig. B.2, that the minimum for the f_4 loss, where $y_{real} = 1$, lies near 0.61, and the minimum for the NGL loss is near 0.57 when $y_{real} = 1$. All losses were used to train ResNet101 model on ImageNet-1k dataset, however, experiments showed that only NGL showed reasonable performance.

Thus, loss NGL was chosen for the experiments on large datasets, such as ImageNet-1k and COCO-Stuff164k, as it doesn't depend on any additional parameters such as ε to make it differentiable, has implicit regularization and showed the best results on small datasets (pre-trained and trained from scratch). Experiments on ImageNet-1k and COCO-Stuff164k showed that found loss function NGL is "slower" compared to CE, for example, as the latter is capable to reach generally good accuracy very quickly. Nevertheless, given the same number of epochs, NGL loss manages to catch up and surpass CE later during the training. It can be caused by the fact that at some point during the training cross-entropy loss stops or barely improves deep learning model's accuracy, while NGL function is more "cautious" during the training due to its implicit regularization, which helps model to prevent overfitting.

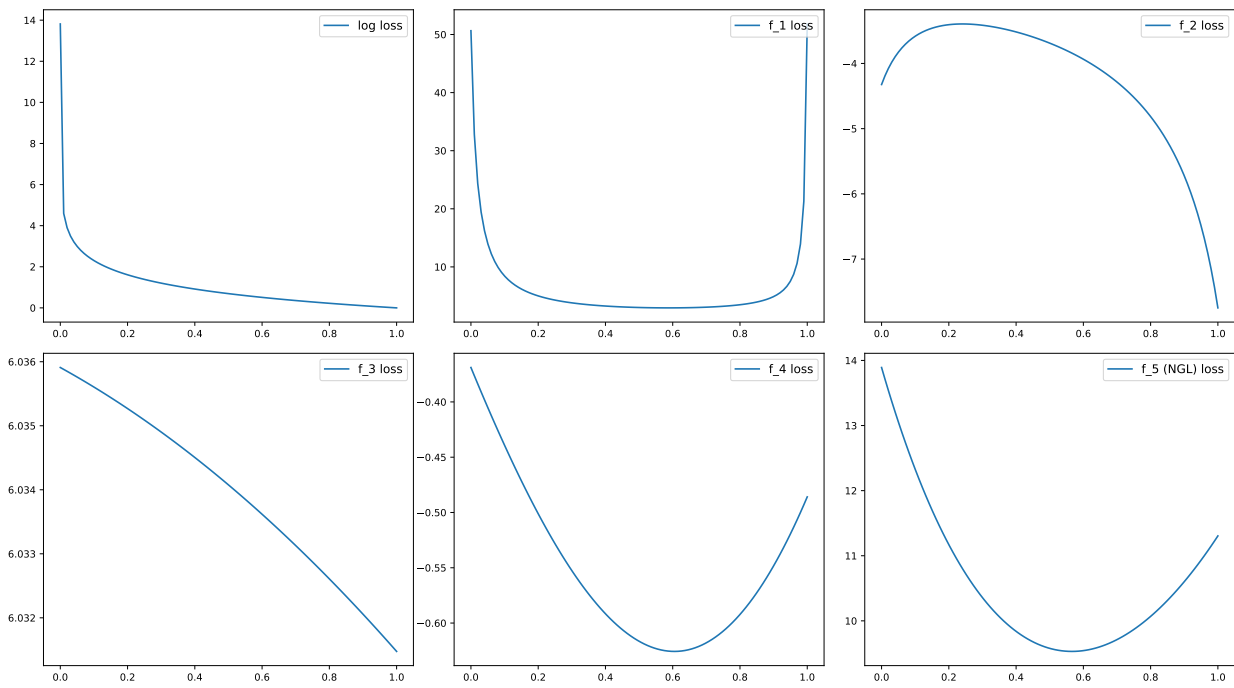


Figure B.2: Functions found by GP and listed in Section 2.1